

Cross-Camera Feature Prediction for Intra-Camera Supervised Person Re-identification across Distant Scenes

Wenhang Ge^{1,2}, Chunyan Pan¹, Ancong Wu^{1,2,*}, Hongwei Zheng⁴, Wei-Shi Zheng^{1,2,3}

¹School of Computer Science and Engineering, Sun Yat-sen University, Guangzhou, China

²Pazhou Lab, Guangzhou, China

³Key Laboratory of Machine Intelligence and Advanced Computing, Ministry of Education, China

⁴University of Chinese Academy of Sciences, Xinjiang, China

gewh@mail2.sysu.edu.cn;panchy8@mail2.sysu.edu.cn;wuanc@mail.sysu.edu.cn;hzheng@ms.xjb.ac.cn;wszheng@ieee.org

ABSTRACT

Person re-identification (Re-ID) aims to match person images across non-overlapping camera views. The majority of Re-ID methods focus on small-scale surveillance systems in which each pedestrian is captured in different camera views of adjacent scenes. However, in large-scale surveillance systems that cover larger areas, it is required to track a pedestrian of interest across distant scenes (e.g., a criminal suspect escapes from one city to another). Since most pedestrians appear in limited local areas, it is difficult to collect training data with cross-camera pairs of the same person. In this work, we study intra-camera supervised person re-identification across distant scenes (ICS-DS Re-ID), which uses cross-camera unpaired data with intra-camera identity labels for training. It is challenging as cross-camera paired data plays a crucial role for learning camera-invariant features in most existing Re-ID methods. To learn camera-invariant representation from cross-camera unpaired training data, we propose a cross-camera feature prediction method to mine cross-camera self supervision information from camera-specific feature distribution by transforming fake cross-camera positive feature pairs and minimize the distances of the fake pairs. Furthermore, we automatically localize and extract local-level feature by a transformer. Joint learning of global-level and local-level features forms a global-local cross-camera feature prediction scheme for mining fine-grained cross-camera self supervision information. Finally, cross-camera self supervision and intra-camera supervision are aggregated in a framework. The experiments are conducted in the ICS-DS setting on Market-SCT, Duke-SCT and MSMT17-SCT datasets. The evaluation results demonstrate the superiority of our method, which gains significant improvements of 15.4 Rank-1 and 22.3 mAP on Market-SCT as compared to the second best method. Our code is available at <https://github.com/g3956/CCFP>.

CCS CONCEPTS

• Computing methodologies → Object identification.

KEYWORDS

person re-identification, self-supervised learning

ACM Reference Format:

Wenhang Ge, Chunyan Pan, Ancong Wu, Hongwei Zheng, Wei-Shi Zheng. 2021. Cross-Camera Feature Prediction for Intra-Camera Supervised Person Re-identification across Distant Scenes. In *Proceedings of the 29th ACM International Conference on Multimedia (MM '21)*, October 20–24, 2021, Virtual Event, China. ACM, New York, NY, USA, 10 pages. <https://doi.org/10.1145/3474085.3475382>

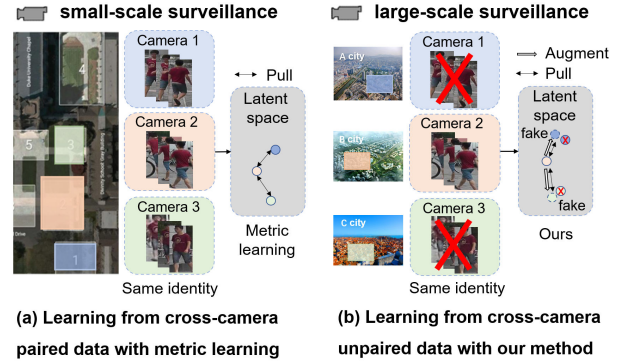


Figure 1: Difference between learning from cross-camera paired data and cross-camera unpaired data. (a) For Re-ID in adjacent scenes, cross-camera paired data can be captured for training. For most existing Re-ID methods, metric learning is performed on such data to learn camera-invariant representation. (b) For Re-ID in distant scenes, it is difficult to capture cross-camera paired data for training. To learn from cross-camera unpaired data in our method, we replace the missing real cross-camera features with transformed fake cross-camera features to mine self supervision information.

1 INTRODUCTION

Person Re-Identification (Re-ID) has been widely investigated as a person retrieval issue across non-overlapping cameras. Given a query person of interest, we aim to retrieve the person who shares the same identity with the query. Due to its great value for social security, Re-ID in large-scale surveillance system is the development trend. Thus, it is imperative to study training method that requires fewer annotations for faster deployment to new scenes.

Most existing Re-ID methods focus on studying training method on a small-scale surveillance system in which each pedestrian is captured in different camera views of adjacent scenes. As shown in Figure 1 (a), these methods perform metric learning on such cross-camera paired data, which is significant for overcoming cross-camera scene variations like viewing angle, background clutter, occlusion and body pose, so that the Re-ID model can learn how the same person appears differently in different cameras to extract camera-invariant representation. When the Re-ID system is extended to a more large-scale one, pedestrian matching is not only required across adjacent scenes but also across distant scenes.

*Corresponding author.

For example, a criminal suspect is escaping across different cities. However, since most pedestrians appear in limited local areas, it is almost impossible for the same pedestrian to be captured in more than one of these distant scenes, so that it is difficult to obtain cross-camera paired training data, as shown in Figure 1 (b). Moreover, annotation for cross-camera pairs also requires massive costs.

One feasible way to reduce the annotation cost is labeling identities within each camera view, which is called intra-camera supervised person Re-ID [26, 62]. However, most existing intra-camera supervised Re-ID methods need to associate underlying cross-camera positive pairs based on training data captured from adjacent scenes with overlapping identities. These methods are hardly applicable to distant scenes in large-scale Re-ID systems [56]. To overcome this limitation, we study intra-camera supervised person Re-ID across distant scenes (ICS-DS Re-ID), which utilizes cross-camera unpaired data with intra-camera identity labels for training. This setting is also called Single Camera Training (SCT) [56], which is still under-explored. Lack of cross-camera paired data incurs a great challenge of how to establish the relation of unpaired samples among different cameras for learning camera-invariant representation.

To address this issue, we propose a Cross-Camera Feature Prediction (CCFP) self-supervised learning framework, which mines cross-camera self supervision information from camera-specific feature distribution to make connection between cross-camera unpaired data. To supplement missing cross-camera paired data in training set, we generate fake cross-camera positive pairs by cross-camera feature augmentation. Then, we regard mapping a feature to its corresponding transformed cross-camera fake feature as cross-camera feature prediction, which can mine cross-camera self supervision information to guide camera-invariant feature learning. Besides learning from global-level features, to further mine fine-grained cross-camera self supervision information, we introduce a transformer to automatically localize and extract local-level features. Joint learning of global-level and local-level features forms a global-local cross-camera feature prediction scheme. Finally, we combine cross-camera self supervision and intra-camera supervision in our framework for learning camera-invariant representation. The main contributions of our work are summarized as follows:

- We propose a cross-camera feature prediction method for mining cross-camera self supervision information to address the problem of lacking cross-camera paired data in the ICS-DS Re-ID setting.
- We further develop a global-local cross-camera feature prediction scheme for mining fine-grained cross-camera self supervision information.
- Extensive experiments on three benchmark datasets show that the proposed framework significantly outperformed the state-of-the-art methods in the ICS-DS Re-ID setting.

2 RELATED WORK

2.1 Fully Supervised Person Re-ID

Fully supervised person Re-ID has made significant progress in recent years based on learning distance metric [7, 22, 31, 47, 48, 54, 59], learning view-invariant discriminative feature [1, 14, 29, 57] or deep learning [4, 25, 27, 28, 33, 38, 41, 53]. However, fully supervised Re-ID requires a large amount of cross-camera identity annotations,

which hinders fast deployment to new scenes. In this work, we investigate intra-camera supervised (ICS) Re-ID, where only intra-camera identity annotations are required, which are easily obtained with off-the-shelf person tracking algorithms [34].

2.2 Intra-Camera Supervised Person Re-ID

In intra-camera supervised (ICS) Re-ID setting, identity labels are independently annotated within each camera and no cross-camera pair is labeled, which reduces the burden of annotation.

Intra-camera supervised Re-ID across adjacent scenes. Most existing ICS Re-ID methods assume that there are underlying overlapping identities across cameras in adjacent scenes in a small-scale surveillance system. This is a problem of intra-camera supervised person re-identification across adjacent scenes (ICS-AS Re-ID). Their main idea is that associating underlying cross-camera positive pairs. TAUDL [26] separately treats each individual camera as a classification task and perform cross-camera positive pairs association. MTML [62] designs a cross-camera multi-label learning under a joint multi-task inference framework for discovering the cross-camera identity correspondence. UGA [52] proposes a graph association method to learn the underlying view-invariant representation. PCSL [36] employs cross-camera soft labels for learning with weighted cross-entropy loss and triplet loss. ACAN [35] combines camera-alignment task and within-camera supervised learning task. TSSL [51] designs a comprehensive learning objective that combines tracklet frame coherence, tracklet neighbourhood compactness, and tracklet cluster structure into a unified framework. Wang *et al.* [46] employ a non-parametric classifier for intra-camera and cross-camera learning.

Intra-camera supervised Re-ID across distant scenes. In this work, we study the problem of intra-camera supervised person re-identification across distant scenes (ICS-DS Re-ID). Different from the assumption of ICS-AS that is valid for small-scale surveillance systems, in large-scale surveillance systems, there is almost no cross-camera paired training data among distant scenes. When learning from cross-camera unpaired data, the ICS-AS Re-ID methods based on underlying cross-camera positive pair association is not reliable, since they associate two cross-camera tracklets with different identities and thus such mismatch results in poor performance. At present, the ICS-DS setting is only investigated in MCNL [56] and still under-explored. MCNL [56] proposes a multi-camera negative loss, which pulls positive pairs closer to the anchor and pushes the within-camera negative pairs further than cross-camera negative pairs. For person Re-ID, alleviating cross-camera intra-class variations is significant but ignored in MCNL. To this end, we propose cross-camera feature prediction to mine cross-camera self supervision information by exploring the relations between transformed fake cross-camera positive pairs to help camera-invariant representation learning.

2.3 Self-Supervised Learning

Self-supervised learning has gained popularity due to its ability to avoid the cost for annotation of large-scale datasets. It can adopt self-defined pseudo labels as supervision for training. Existing self-supervised learning methods can be categorized into three general types. First, generative self-supervised learning [10, 11, 21, 37] aims

to train an encoder to encode input \mathbf{x} into a hidden representation \mathbf{z} and a decoder to reconstruct \mathbf{x} from \mathbf{z} . Contrastive self-supervised learning [3, 5, 6, 15, 16, 42] aims to train an encoder by pulling the embeddings of the same sample with different data augmentation closer while pushing embeddings of other samples away. Adversarial self-supervised learning [12, 13, 23, 24] aims to generate fake samples by training a generator and distinguish them from real samples by a discriminator. Currently, contrastive self-supervised learning has become dominant in computer vision. However, data augmentation strategy in current self-supervised learning methods is not specific for person Re-ID task and cannot reflect cross-camera intra-class variations. In our method, cross-camera feature augmentation is camera-aware augmentation in feature level, which can help learning camera-invariant features.

3 APPROACH

3.1 Formulation

A set of person images is collected and denoted by $\mathcal{X} = \{\mathcal{X}^c\}_{c=1}^C$, where $c \in \{1, \dots, C\}$ denotes the camera label. In the setting of intra-camera supervised (ICS) Re-ID, the image-label pairs of camera c are denoted by $\mathcal{X}^c = \{(\mathbf{x}_i^c, y_i^c)\}_{i=1}^{N_c}$, where \mathbf{x}_i^c is image and y_i^c is the corresponding intra-camera identity label and N_c is the number of samples. In the real world applications in large-scale surveillance systems, both matching between adjacent scenes and matching between distant scenes are required. We categorize ICS setting into intra-camera supervised Re-ID across adjacent scenes (ICS-AS) and intra-camera supervised Re-ID across distant scenes (ICS-DS). In this work, we study the under-explored ICS-DS setting, in which cross-camera positive pair does not exist in training data captured in distant scenes, i.e., $y_i^{c_1} \neq y_j^{c_2}$ for all i, j and $c_1 \neq c_2$. In comparison, the ICS-AS setting is studied in most existing ICS Re-ID methods, in which training data with a large number of underlying cross-camera positive pairs are captured in adjacent scenes, i.e., there exist i, j and $c_1 \neq c_2$ that satisfy $y_i^{c_1} = y_j^{c_2}$.

We aim to train a feature extractor $H(\cdot; \Theta)$ parameterized by Θ on \mathcal{X} to extract discriminative feature $\mathbf{f}_i^c = H(\mathbf{x}_i^c; \Theta) \in \mathbb{R}^d$ for image \mathbf{x}_i^c to match.

3.2 Cross-Camera Feature Prediction

3.2.1 Cross-Camera Feature Augmentation. For person Re-ID task, the learning objective of feature extractor $H(\cdot; \Theta)$ is

$$\mathcal{D}(\mathbf{f}_a^{c_a}, \mathbf{f}_p^{c_p}) < \mathcal{D}(\mathbf{f}_a^{c_a}, \mathbf{f}_n^{c_n}), \quad (1)$$

where \mathcal{D} is a distance metric, $\mathbf{f}_a^{c_a}, \mathbf{f}_p^{c_p}, \mathbf{f}_n^{c_n}$ are anchor feature from camera c_a , positive feature from camera c_p and negative feature from camera c_n , respectively. The objective requires the distance between positive pairs to be smaller than that between negative pairs. With the distance between cross-camera positive pair $\mathbf{f}_a^{c_a}, \mathbf{f}_p^{c_p}$ ($c_a \neq c_p$) minimized, cross-camera scene variations can be eliminated, which is helpful for learning discriminative representation.

However, in the ICS-DS setting, there is nearly no cross-camera positive pair in training data. For an anchor feature $\mathbf{f}_a^{c_a}$, we can hardly find a $\mathbf{f}_p^{c_p}$ of a different camera ($c_a \neq c_p$), which makes it difficult to model intra-class cross-camera scene variations. For ICS-DS Re-ID, Zhang *et al.* [56] have experimentally shown that

traditional metric learning loss results in dramatic performance degradation with a cross-camera unpaired training set. How to establish the relation of cross-camera unpaired data is the key.

To overcome this problem, we replace the missing real cross-camera positive pair $\mathbf{f}_a^{c_a}, \mathbf{f}_p^{c_p}$ ($c_a \neq c_p$) with fake cross-camera positive pair $\mathbf{f}_a^{c_a}, \hat{\mathbf{f}}_p^{c_p}$ ($c_a \neq c_p$). Fake feature $\hat{\mathbf{f}}_p^{c_p}$ is obtained by

$$\hat{\mathbf{f}}_p^{c_p} = \text{Augment}(\mathbf{f}_a^{c_a}, c_p), \quad (2)$$

where Augment is a transformation for feature $\mathbf{f}_a^{c_a}$ from camera c_a to camera c_p . With the transformed fake feature, the learning objective in Eq. (1) becomes:

$$\mathcal{D}(\mathbf{f}_a^{c_a}, \hat{\mathbf{f}}_p^{c_p}) < \mathcal{D}(\mathbf{f}_a^{c_a}, \mathbf{f}_n^{c_n}). \quad (3)$$

To realize this learning objective, we aim to design a transformation function and further design loss functions to explore the relation between transformed features, which can be regarded as scheme of mining self supervision information. Variations of lighting, viewpoint and background lead to camera-specific image style for Re-ID. Since person images captured from different cameras are of different image styles and the image styles are camera-specific, we assume the feature distribution of each camera follows a camera-specific Gaussian distribution, which is denoted as $\{N(\boldsymbol{\mu}_c, \boldsymbol{\sigma}_c^2)\}_{c=1}^C$.

We note that Batch Normalization (BN) layer [19] can estimate the moment statistics (i.e., mean and variance) of feature distribution and normalize features to normal distribution. To realize the transformation, we propose a cross-camera feature augmentation module that consists of C camera-specific Batch Normalization (CSBN) layers [64], each of which estimates the camera-specific moment statistics $\{\boldsymbol{\mu}_c, \boldsymbol{\sigma}_c^2\}$. Given a set of features of camera c denoted as $\{\mathbf{f}_i^c\}_{i=1}^{N_c}$, CSBN estimates camera-specific mean and variance by

$$\boldsymbol{\mu}_c = \frac{1}{N_c} \sum_{i=1}^{N_c} \mathbf{f}_i^c, \quad \boldsymbol{\sigma}_c^2 = \frac{1}{N_c} \sum_{i=1}^{N_c} (\mathbf{f}_i^c - \boldsymbol{\mu}_c)^2, \quad (4)$$

where $\boldsymbol{\mu}_c$ and $\boldsymbol{\sigma}_c$ are the camera-specific mean and variance.

Given a feature \mathbf{f}_i^c of camera c , we transform it to a fake feature in the camera-specific distribution of a different camera c' by

$$\hat{\mathbf{f}}_i^{c'} = \text{Augment}(\mathbf{f}_i^c, c') = \gamma \frac{\mathbf{f}_i^c - \boldsymbol{\mu}_{c'}}{\sqrt{\boldsymbol{\sigma}_{c'}^2 + \epsilon}}, \quad (5)$$

where γ and β are two parameters learned during training. ϵ is a small value to keep stability.

It is called *cross-camera feature augmentation* as shown on the left of Figure 2. After this transformation, the feature \mathbf{f}_i^c of camera c is mapped to the distribution of camera c' as shown on the right of Figure 2. The relation between feature $\hat{\mathbf{f}}_i^{c'}$ and feature \mathbf{f}_i^c contains self supervision information of camera-specific feature distribution, which requires to be further mined.

Discussion. To model camera-specific feature distribution, both CBN [63, 64] for generalizable Re-ID and CSBN in our method exploit camera-specific batch normalization (BN) components, which are applied in different ways for different purposes. In CBN [63, 64], camera-specific BN operates on samples of the corresponding camera for distribution alignment; in our method, camera-specific BN operates on samples of all cameras to augment cross-camera fake

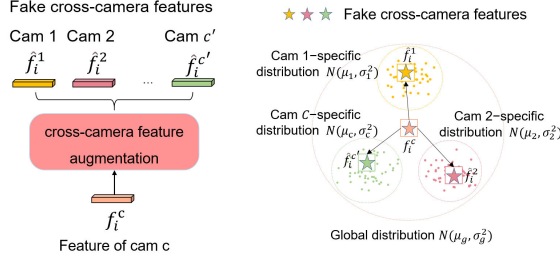


Figure 2: Cross-Camera feature augmentation.

features for further mining cross-camera self supervision information that is ignored by CBN [63, 64].

3.2.2 Predicting Cross-Camera Fake Feature. The relation between transformed cross-camera features contain self supervision information of camera-specific distribution. To mine cross-camera self supervision information for camera-invariant representation learning, we propose a *cross-camera feature prediction* scheme as shown in Figure 3.

We assume the features of all cameras follow a global Gaussian distribution. Similar to the camera-specific BN, we apply a BN layer called global BN on f_i^c to obtain a normalized feature $f_i^{c, glo}$, which is also the feature for inference in the testing stage. For each sample x_i as input, we can obtain $C + 1$ views of features, including a normalized feature $f_i^{c, glo}$ and fake cross-camera features $\{\hat{f}_i^{c'}\}_{c'=1}^C$. Since all of them are encoded from the same image x_i , we regard these features of different camera-specific views share the same identity. For a fake cross-camera positive pair of feature f_i^c and feature $\hat{f}_i^{c'}$, we expect that f_i^c can be used to predict $\hat{f}_i^{c'}$ by mapping f_i^c to $\hat{f}_i^{c'}$ in a global distribution, which can be formulated by

$$\mathcal{L} = \frac{1}{N} \frac{1}{C} \sum_{i=1}^N \sum_{c'=1}^C \mathcal{D}(f_i^{c, glo}, \text{stop-gradient}(\hat{f}_i^{c'})), \quad (6)$$

where $\hat{f}_i^{c'}$ is regarded as the prediction target so that stop-gradient is applied to it. \mathcal{D} is cosine distance.

However, the formulation in Eq. (6) only takes fake features transformed from a single feature into account, while intra-camera supervision is ignored, which is crucial for alleviating intra-class variations. Thus, we also minimize the distances between $f_i^{c, glo}$ and cross-camera features of the same intra-camera identity with $f_i^{c, glo}$, in order to alleviate the effect of both cross-camera scene variations and intra-class variations. To achieve this, we formulate a Global Self-supervised Loss (GSL) as follow:

$$\mathcal{L}_{GSL} = \frac{1}{N} \frac{1}{C} \frac{1}{|\mathcal{P}_i|} \sum_{i=1}^N \sum_{j \in \mathcal{P}_i} \mathcal{D}(f_i^{c, glo}, \text{stop-gradient}(\hat{f}_j^{c'})), \quad (7)$$

where \mathcal{P}_i denotes the set of indices of samples that share the same identity with x_i (i.e., $y_i = y_j$) and $|\mathcal{P}_i|$ is the cardinality of \mathcal{P}_i .

This is called *cross-camera feature prediction*. By minimizing the distances between the fake cross-camera positive pairs, self supervision information in camera-specific feature distribution is mined and used to guide camera-invariant feature learning.

Discussion. The commonly used distribution alignment methods, such as MMD [32] and CORAL [40] and HHL [61], model the relation between different domains by minimizing distribution distance, while instance-level relation is ignored. By contrast, our method models the relation between different domains by fake cross-camera positive pairs in instance level, which is exploiting self supervision information mined from domain-specific distributions. Such instance-level modeling is significant for alleviating intra-class variations and thus is more suitable for Re-ID task.

3.3 Global-Local Cross-Camera Feature Prediction Scheme

The global self-supervised loss exploits global-level features extracted from the whole image for self-supervised learning. To extract more fine-grained features to complement global-level self-supervised learning, we further propose a global-local cross-camera feature prediction scheme, which aggregates fine-grained local-level feature with global-level feature. We expect that our model can automatically localize local regions from the feature map based on contextual information and then perform self-supervised learning in local level to mine fine-grained self supervision information. To this end, we employ a Transformer [44] which can effectively model contextual information for local self-supervised learning in our cross-camera feature prediction scheme.

Local Feature Extraction by Transformer. Motivated by DETR [2], we apply a transformer for extracting local-level features of multiple local regions on feature map $z_i \in \mathbb{R}^{d \times H \times W}$ extracted by the backbone model. The transformer consists of an encoder $E(\cdot; \Theta_E)$ for learning contextual information and a decoder $D(\cdot; \Theta_D)$ for localizing region of interest based on contextual information for local-level feature extraction. We resize the feature map $z_i \in \mathbb{R}^{d \times H \times W}$ to obtain $z_i \in \mathbb{R}^{d \times HW}$ as the input of encoder. The output embedding of the encoder $z_i^e \in \mathbb{R}^{d \times HW}$ is

$$z_i^e = E(z_i; \Theta_E). \quad (8)$$

The decoder takes z_i^e as input and finally outputs P local-level features:

$$\{w_i^p\}_{p=1}^P = D(z_i^e; \Theta_D). \quad (9)$$

As for the detailed architecture for the transformer, we follow the design in DETR [2].

Local-level Self-Supervised Learning. Since local-level feature contains more fine-grained information, to exploit local-level feature for self-supervised learning, we propose a Local-level Self-supervised Loss (LSL). Similar to the model architecture used in global-level self-supervised learning, we apply another local cross-camera feature augmentation module and global BN after the backbone in the feature map level as shown in Figure 3 (b). The feature map z_i^c output by the backbone is further input to the global BN and the local cross-camera augmentation module to get a normalized feature map $z_i^{c, glo}$ and cross-camera feature maps $\{\hat{z}_i^{c'}\}_{c'=1}^C$, $i \in (1, 2, \dots, N)$, respectively. We assimilate the idea of global-level self-supervised learning into local-level learning. Specifically, We input $z_i^{c, glo}$ and $\{\hat{z}_i^{c'}\}_{c'=1}^C$, $i \in (1, 2, \dots, N)$ into the Transformer to extract local-level features. For each feature map z_i^c as input, P

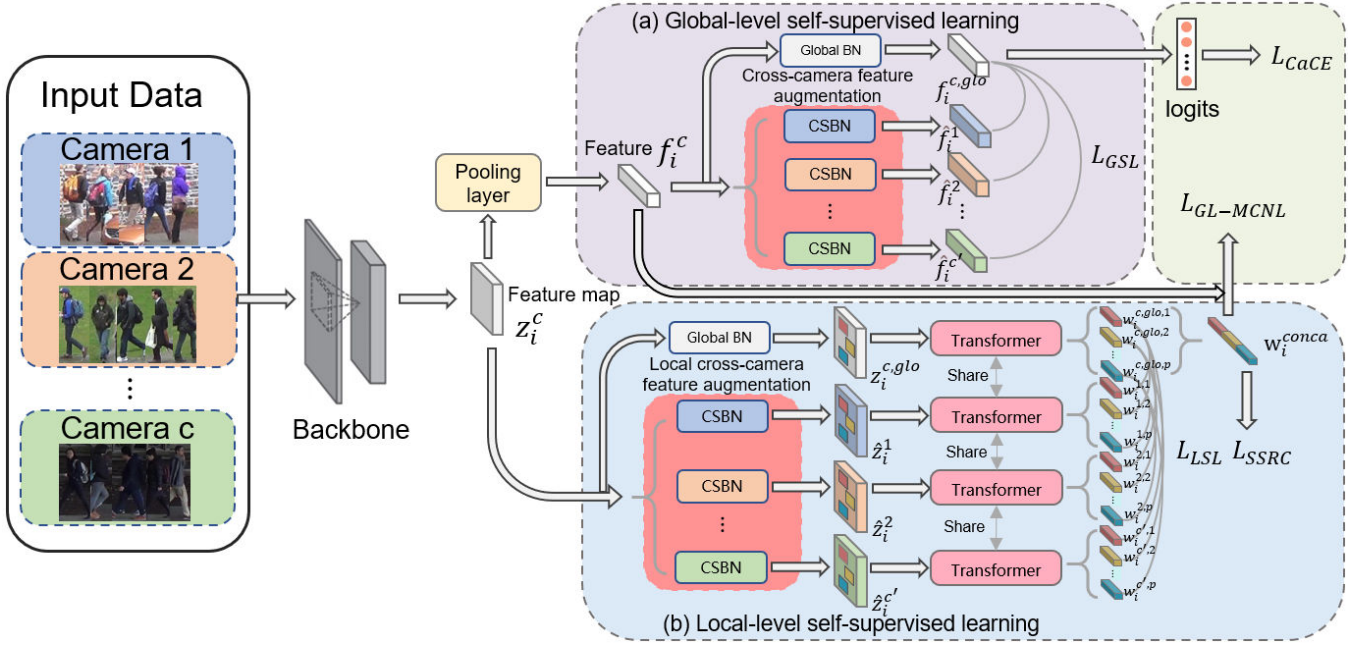


Figure 3: An overview of our framework. The cross-camera feature prediction scheme for mining cross-camera self supervision information is composed of (a) global-level self-supervised learning and (b) local-level self-supervised learning. In (a), GSL is designed to minimize the distances between features of the same intra-camera identity label, including $f_i^{c, glo}$ output by global BN and the corresponding cross-camera features \hat{f}_i^c , $c \in (1, 2, \dots, C)$. In (b), LSL is designed to minimize the distance between features $w_i^{c, glo, p}$ and $w_i^{c', p}$ of each local region. SSRC loss is a regularization term for guiding multiple local region learning. Finally, camera-aware cross entropy loss and GL-MCNL loss are employed for representation learning with intra-camera supervision.

local-level features $\{w_i^{c, p}\}_{p=1}^P$ are output by the transformer. Similar to the GSL, we enforce each local-level feature $w_i^{c, glo, p}$ of $z_i^{c, glo}$ and $w_i^{c', p}$ of corresponding cross-camera feature maps $\hat{z}_i^{c'}$ for each sample to be pulled close in the embedding space:

$$\mathcal{L}_{LS} = \frac{1}{N} \frac{1}{C} \frac{1}{P} \sum_{i=1}^N \sum_{c=1}^C \sum_{p=1}^P \mathcal{D} \left(w_i^{c, glo, p}, \text{stop-gradient}(w_i^{c', p}) \right). \quad (10)$$

To guide multiple local region learning, we introduce a shared-specific region constraint (SSRC) loss as a regularization term, which consists of a specific loss and a shared loss as follows.

On the one hand, we expect that different regions can focus on different parts with large appearance variations to extract part-specific features. To this end, we employ specific loss to push local-level features $\{w_i^{c, glo, p}\}_{p=1}^P$, $i \in (1, 2, \dots, N)$ away from each other formulated as follow:

$$\mathcal{L}_{specific} = - \sum_{i=1}^N \sum_{p=1}^P \log \frac{\exp \left(s \left(w_i^{c, glo, p}, w_i^{c, glo, p} \right) \right)}{\sum_{q=1}^P \exp \left(s \left(w_i^{c, glo, p}, w_i^{c, glo, q} \right) \right)}, \quad (11)$$

where $s(\cdot)$ measures the cosine similarity between two features.

On the other hand, we also expect each region can focus on some shared patterns of different persons to avoid attending to

person-irrelevant regions. We regard region index p as class label and employ Softmax cross entropy loss to classify the feature as follow:

$$\mathcal{L}_{share} = - \sum_{i=1}^N \sum_{p=1}^P C_i^p \log q_i^{c, glo, p}, \quad (12)$$

where C_i^p is a one-hot vector representing the index p and $q_i^{c, glo, p}$ is the output logit of fully connected layer with softmax operation. In summary, The SSRC loss is formulated as:

$$\mathcal{L}_{SSRC} = \mathcal{L}_{specific} + \mathcal{L}_{share}. \quad (13)$$

Finally, the total loss for local-level self-supervised learning is:

$$\mathcal{L}_{LSL} = \mathcal{L}_{LS} + \mathcal{L}_{SSRC}. \quad (14)$$

3.4 An ICS-DS Re-ID Framework

To learn from intra-camera identity labels in the ICS-DS setting, we adopt the commonly used classification loss and metric learning loss and further aggregate cross-camera self supervision and intra-camera supervision into our ICS-DS Re-ID framework.

Global-local MCNL. For discriminative feature learning, we apply a metric learning loss MCNL [56] that is designed for ICS-DS setting. MCNL loss exploits intra-camera pairs and cross-camera

negative pairs for learning from intra-camera supervision information, which is complementary to our cross-camera feature prediction that exploits fake cross-camera positive pairs to learn from cross-camera self supervision information.

For each feature map $z_i^{c, glo}$, we concatenate the local-level features $\left\{w_i^{c, glo, p}\right\}_{p=1}^P$ output by Transformer to obtain a combined local-level feature w_i^{conca} . We apply MCNL loss on both global-level feature f_i^c and local-level feature w_i^{conca} to formulate a global-local MCNL (GL-MCNL) loss formulated by:

$$\begin{aligned} \mathcal{L}_{GL-MCNL} = & \frac{1}{N} \sum_{* \in \{glo, loc\}} \sum_{i=1}^N \left[m_1 + \text{dist}_{+, intra}^{*, i} - \text{dist}_{-, cross}^{*, i} \right]_+ \\ & + \left[m_2 + \text{dist}_{-, cross}^{*, i} - \text{dist}_{-, intra}^{*, i} \right]_+, \end{aligned} \quad (15)$$

where $[z]_+ = \max(z, 0)$, $\text{dist}_{+, intra}^{*, i}$ denotes distance between anchor and within-camera hard positive pair. $\text{dist}_{-, cross}^{*, i}$ denotes distance between anchor and cross-camera hard negative pair. $\text{dist}_{-, intra}^{*, i}$ denotes distance between anchor and intra-camera hard negative pair. $* \in \{glo, loc\}$ denotes distance calculated by global-level feature and local-level feature, respectively.

Camera-aware Cross Entropy Loss. We assimilate the main idea of MCNL to formulate a new camera-aware cross entropy (CaCE) loss. CaCE loss is formulated as:

$$\mathcal{L}_{CE} = - \sum_{i=1}^C p_i \log q_i, \quad (16)$$

where q_i is the output logits of sample x_i representing the possibilities of classes and p_i is the ground truth soft label formulated as:

$$p_i = \begin{cases} 1 - \varepsilon & \text{if } i = j \\ -\varepsilon / (K_e - 1) & \text{if } i \neq j \wedge c_i \neq c_j \\ \varepsilon / (K_n - 1) & \text{if } i \neq j \wedge c_i = c_j \end{cases}, \quad (17)$$

where c_i is the camera label of sample x_i . K_e is the number of classes whose camera label is the same with c_i and K_n is the number of class whose camera label is different from c_i . ε is set as 0.1.

Finally, our framework is learned with joint guidance of cross-camera self supervision and intra-camera supervision by

$$\mathcal{L}_{CCFP} = \mathcal{L}_{CaCE} + \mathcal{L}_{GL-MCNL} + \mathcal{L}_{GSL} + \mathcal{L}_{LSL}. \quad (18)$$

During testing, we only use features f_i^c output by global BN in Figure 3 (a) for testing, which can save computation costs.

4 EXPERIMENTS

4.1 Datasets and Evaluation Protocol

To evaluate the effectiveness of our model, we conducted experiments in the ICS-DS setting on three benchmark person Re-ID datasets, Market-SCT, DukeMTMC-SCT and MSMT17-SCT, which are modified from Market-1501 [57], DukeMTMC [60] and MSMT17 [49] following the data split in single camera training (SCT) [56], because existing datasets do not meet the requirement of having cross-camera unpaired training data. Compared with the original dataset, we randomly select images of one camera for each identity to construct the training set and keep the original testing data and testing protocols unchanged. The details of datasets used in our

Table 1: Details of datasets used in our experiments.

Dataset	Train IDs	Train Images	Test IDs	Test Images	cross-camera paired data
Market-1501	751	12936	750	15913	True
Market-SCT	751	3561	750	15913	False
DukeMTMC	702	16522	1110	17661	True
Duke-SCT	702	5993	1110	17661	False
MSMT17	1041	32621	3060	93820	True
MSMT-SCT	1041	6645	3060	93820	False

experiments are shown in Table 1. The evaluation metrics are the Rank-k accuracy and the mean average precision (mAP)[58].

4.2 Implementation Details

ResNet-50 [17] pre-trained on ImageNet [8] was adopted as our backbone. The details of its structure followed the design in AGW [55]. For local-level feature extraction, a 1x1 convolution was used to reduce the channel dimension of the feature map z_i^c output by the backbone to a smaller dimension of 256 before it was input to Transformer. The parameters of Transformer in local-level self-supervised learning followed DETR [2], except that the number of local regions P was set as 12 empirically. The feature output by pooling layer was used for metric learning. The data augmentation strategy followed the implementation in fast-reid [18]. The mini-batch size was 128. As for mini-batch sampling strategy, we randomly selected images from 2 cameras. We used Adam [20] as our optimizer, and the learning rate was set to 0.0006 initially and decayed by 0.1 every 100 epochs in 300 epochs totally.

4.3 Comparison with State-of-the-Art Methods

We evaluated several methods including the state-of-the-art intra-camera supervised methods, fully supervised learning methods, self-supervised learning methods, metric learning methods and distribution alignment methods. The results are shown in Table 2.

Intra-camera supervised (ICS) methods. We categorize ICS Re-ID methods into ICS-AS methods and ICS-DS methods.

- **ICS-AS methods.** We compared with methods for intra-camera supervised Re-ID across adjacent scenes (ICS-AS) including TAULD [26], TSSL [51], MTML [62], UGA [52], PCSL [36] and Precise-ICS [46]. They were designed for small-scale surveillance systems and their training set included underlying cross-camera positive pairs. Since Precise-ICS [46] achieved best performance in the ICS-AS setting, we implemented it in the ICS-DS setting. For other methods, we used their results in the ICS-AS setting reported in their original papers. Compared with ICS-AS setting, ICS-DS setting is more challenging without cross-camera paired training data, but our method still surpassed the ICS-AS Re-ID methods on Duke-SCT and MSMT-SCT. Moreover, our method clearly outperformed Precise-ICS in the same ICS-DS setting.

- **ICS-DS methods.** We compared with the state-of-the-art ICS-DS Re-ID method MCNL [56]. We outperformed MCNL by a large margin, which gains improvement of 15.4 Rank-1 and 22.3 mAP on Market-SCT, 13.2 Rank-1 and 19.3 mAP on Duke-SCT, 23.5 Rank-1,

Setting	Methods	Reference	Duke-SCT				Market-SCT				MSMT17-SCT			
			R-1	R-5	R-10	mAP	R-1	R-5	R-10	mAP	R-1	R-5	R-10	mAP
ICS-AS	ICS													
	TAULD [§] [26]	ECCV 18	61.7	-	-	43.5	63.7	-	-	41.2	-	-	-	-
	TSSL [§] [51]	AAAI 20	62.2	-	-	38.5	71.2	-	-	43.3	-	-	-	-
	MTML [§] [62]	ICCV 19	71.7	-	86.9	50.7	85.3	-	96.2	65.2	44.1	-	63.9	18.6
	UGA [§] [52]	ICCV 19	75.0	-	-	53.3	87.2	-	-	70.3	49.5	-	-	21.7
	PCSL [§] [36]	TCSVT20	71.7	84.7	88.2	53.5	87.0	94.8	96.6	69.4	48.3	62.8	68.6	20.7
ICS-DS	Fully Supervised													
	PCB [41]	ECCV 18	32.7	-	-	22.2	43.5	-	-	23.5	-	-	-	-
	Suh’s method [39]	ECCV 18	38.5	-	-	25.4	48.0	-	-	27.3	-	-	-	-
	MGN-ibn [45]	ACMMM’ 18	46.7	59.8	67.1	32.6	45.6	61.2	69.3	26.6	27.8	38.6	44.1	11.7
	bagtricks [33]	CVPR 19	54.2	68.9	76.7	42.0	54.0	71.3	78.4	34.0	20.4	31.0	37.2	9.8
	AGW [55]	TPAMI 21	56.5	71.0	77.7	43.9	56.0	72.3	79.1	36.6	23.0	33.9	40.0	11.1
	Metric Learning													
	Center Loss [50]	ECCV 16	38.7	-	-	23.3	40.3	-	-	18.5	-	-	-	-
	A-Softmax [30]	CVPR 17	34.8	-	-	22.9	41.9	-	-	23.2	-	-	-	-
	ArcFace [9]	CVPR 19	35.8	-	-	22.8	39.4	-	-	19.8	-	-	-	-
	Self-supervised													
	HHL [†] [61]	ECCV 18	50.3	64.0	70.3	33.0	65.6	80.6	86.8	44.8	31.4	42.5	48.1	11.0
	SimSiam [6]	CVPR 21	28.1	43.2	51.3	19.7	36.2	51.9	59.1	18.0	2.8	5.9	8.4	1.2
	Distribution alignment													
	MMD [32]	JMLR 15	74.1	85.9	90.2	56.3	67.7	83.1	88.2	44.0	42.2	55.8	61.4	18.2
	CORAL [40]	ECCV 16	76.8	87.1	90.0	59.7	76.2	88.5	93.0	51.5	42.6	55.8	61.5	19.5
	ICS													
Precise-ICS [46]	WACV 21	41.2	57.9	64.2	25.9	50.0	67.5	74.8	31.2	17.2	28.4	34.3	6.7	
MCNL [‡] [56]	AAAI 20	67.1	80.9	84.7	45.2	67.0	82.8	87.9	41.6	26.6	40.0	46.4	10.0	
CCFP(ours)	ours	80.3	89.0	91.9	64.5	82.4	92.6	95.4	63.9	50.1	63.3	68.8	22.2	

Table 2: Comparison with state-of-the-art methods on Duke-SCT, Market-SCT and MSMT17-SCT. R-k denotes Rank-k accuracy (%) and mAP denotes mean average precision (%). MCNL[‡] [56]: We used the code released by the authors and achieved higher performance than that reported in the paper. § TAULD [26], TSSL [51], MTML [62], UGA [52] PCSL [36]: ICS Re-ID models trained with cross-camera paired data in the ICS-AS setting. HHL[†]: we modified unsupervised HHL as an intra-camera supervised version. Results in bold font denote the best performance in the ICS-DS setting.

because our method further exploits cross-camera self supervision information which is ignored in MCNL.

Self-supervised learning methods. For comparison with self-supervised learning methods, we chose representative contrastive self-supervised learning method SimSiam [6] and adversarial self-supervised learning method HHL [61] that is specific for Re-ID. For fair comparison, we modified unsupervised HHL as an intra-camera supervised version denoted as HHL[†]. Specifically, intra-camera positive pairs as well as their generated images shared the same label. We outperformed these two representative self-supervised methods by a large margin. The effectiveness of HHL is restricted by the quality of generated images. SimSiam ignores camera-specific distribution of person Re-ID. In comparison, our cross-camera feature augmentation can model cross-camera relation more effectively.

Distribution alignment methods. Since our proposed method is closely related with distribution alignment methods, we also compared two commonly used distribution alignment losses Maximum Mean Discrepancy (MMD) loss [32] and CORAL loss [40]. For fair comparison, both losses were applied based on our baseline. Our method still outperformed them, because our method models the relation between different domains by cross-camera features in

Table 3: Ablation study on individual components of CCFP. “CaCE” denotes camera-aware cross entropy loss. “GSL” denotes global-level self-supervised learning loss. “LSL” denotes local-level self-supervised learning loss. “SSRC” denotes shared-specific region constraint loss.

Methods	Market-SCT		Duke-SCT	
	R-1	mAP	R-1	mAP
baseline	75.7	51.5	70.1	53.1
+ CaCE	77.6	52.3	71.4	54.6
+ CaCE + GSL	78.9	59.5	75.7	60.4
+ CaCE + GSL + LSL (w/o SSRC)	80.5	61.4	78.7	62.7
+ CaCE + GSL + LSL (full model)	82.4	63.9	80.3	64.5

instance level. While commonly used distribution alignment loss only considers the global distribution distances.

4.4 Ablation Study

We performed ablation study to evaluate the effectiveness of each component in our model. The experimental results are reported in Table 3. “+” means combining the component with baseline.

The effectiveness of GSL. Compared with “+ CaCE”, the performance of “+ CaCE + GSL” was clearly improved on both datasets.

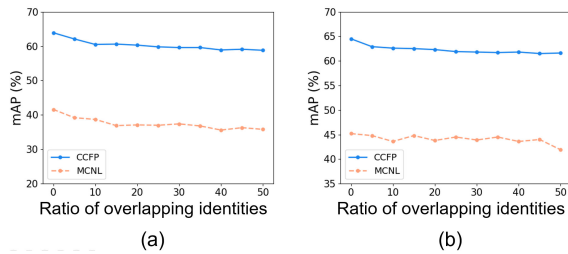


Figure 4: Analysis on ratio of overlapping identities. (a) Comparison between CCFP and MCNL on Market-1501. (b) Comparison between CCFP and MCNL on DukeMTMC.

This indicates that global-level self-supervised learning can effectively mine cross-camera self supervision information to eliminate cross-camera scene variations without cross-camera positive pairs.

The effectiveness of LSL. Compared with “+ CaCE + GSL”, the performance of “+ CaCE + GSL + LSL” is clearly improved, which indicates that the fine-grained self supervision information can complement global-level self-supervised learning.

The effectiveness of SSRC. Compared with “+ CaCE + GSL + LSL”, the performance of “+ CaCE + GSL + LSL (w/o SSRC)” dropped, which indicates that more diverse local-level feature can facilitate local-level self-supervised learning.

The effectiveness of CaCE. Compared with “baseline” which employed traditional cross entropy loss, the performance of our camera-aware cross entropy “+ CaCE” was improved on both datasets, which indicates CaCE is more effective in ICS-DS setting.

4.5 Further Analysis

The impact of cross-camera identity overlap ratio. We also consider the situations between ICS-DS setting and ICS-AS setting. Since in real-world large-scale surveillance systems, matching between scenes of different distances are required, i.e., there are different ratios of overlapping identities across different cameras. We additionally simulate different ratios of overlapping identities.

To evaluate our method in this setting, we reconstructed the training set on Market-1501 and DukeMTMC with different ratios of overlapping identities from 5% to 50% with increment of 5% in each step. The state-of-the-art ICS-DS Re-ID method MCNL was compared. The results are shown in Figure 4. The results demonstrate that our method was robust to identity overlap ratios, because our method does not rely on cross-camera overlapping identities. Moreover, our method outperformed MCNL by a large margin.

The impact of number of local regions P . The number of local regions determines how many local-level features are output by the Transformer. The results are reported in Figure 5. We varied P from 2 to 16. When P was increased from 2 to 12, the performance kept increasing because more diverse fine-grained local-level features can be extracted for local-level self-supervised learning. When P was larger than 12, we observed a drop of performance, since excessive local regions make local-level features become redundant.

Visualization. To better understand the effect of cross-camera feature prediction as for self supervision information mining and learning, we visualized the feature distribution learned by the baseline model and our method as shown in Figure 6. From figure 6

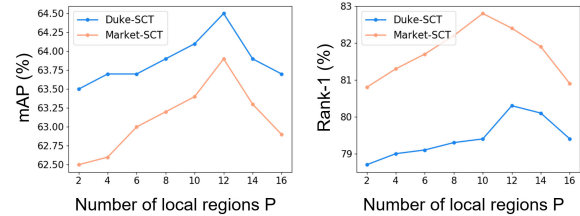


Figure 5: Analysis on the number of local regions P .

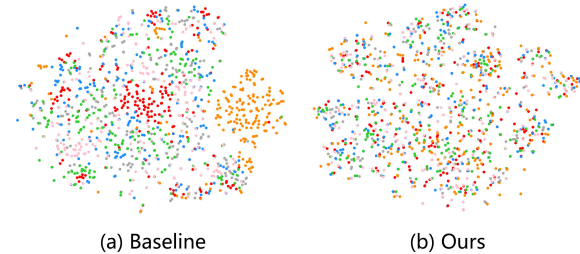


Figure 6: t-SNE visualization [43] of feature distribution from a subset of Market-1501. Best viewed in color.

we can observe that, the camera-specific distribution of baseline is not identical, which is harmful for cross-camera matching, while our method achieves more identical camera-specific distribution, which is favorable for cross-camera matching.

5 CONCLUSION

In this paper, we investigate intra-camera supervised person re-identification across distant scenes (ICS-DS Re-ID), which is significant for large-scale video surveillance systems but remains under-explored. Lack of cross-camera paired data leads to a challenge of how to establish the relation of unpaired samples among different cameras, which is ignored by most intra-camera supervised person re-identification methods. To overcome this issue, we propose a cross-camera feature prediction (CCFP) to mine cross-camera self supervision information from camera-specific distributions by transforming fake cross-camera positive features based on camera-specific batch normalization layers. Furthermore, to capture more fine-grained cross-camera self supervision information, we employ transformer to automatically localize and extract local-level features for local-level self-supervised learning. Finally, cross-camera self supervision and intra-camera supervision are aggregated into an unified framework for camera-invariant representation learning. Extensive experiments on Market-SCT, Duke-SCT and MSMT17-SCT in the ICS-DS setting validate the superiority of our method.

ACKNOWLEDGEMENT

This work was partially supported by NSFC (U1911401, U1811461), China National Postdoctoral Program for Innovative Talents (BX2020 0395), China Postdoctoral Science Foundation (2021M693616), Guangdong NSF Project (No. 2020B1515120085, 2018B030312002), and the Key-Area Research and Development Program of Guangzhou (202007030004).

REFERENCES

- [1] Loris Bazzani, Marco Cristani, and Vittorio Murino. 2013. Symmetry-driven accumulation of local features for human characterization and re-identification. *Computer Vision and Image Understanding (CVIU)* (2013).
- [2] Nicolas Carion, Francisco Massa, Gabriel Synnaeve, Nicolas Usunier, Alexander Kirillov, and Sergey Zagoruyko. 2020. End-to-end object detection with transformers. In *European Conference on Computer Vision (ECCV)*. Springer.
- [3] Mathilde Caron, Ishan Misra, Julien Mairal, Priya Goyal, Piotr Bojanowski, and Armand Joulin. 2020. Unsupervised learning of visual features by contrasting cluster assignments. *arXiv preprint arXiv:2006.09882* (2020).
- [4] Tianlong Chen, Shaojin Ding, Jingyi Xie, Ye Yuan, Wuyang Chen, Yang Yang, Zhou Ren, and Zhangyang Wang. 2019. Abd-net: Attentive but diverse person re-identification. In *Proceedings of the IEEE International Conference on Computer Vision (CVPR)*.
- [5] Ting Chen, Simon Kornblith, Mohammad Norouzi, and Geoffrey Hinton. 2020. A simple framework for contrastive learning of visual representations. In *International conference on machine learning (ICML)*. PMLR.
- [6] Xinlei Chen and Kaiming He. 2020. Exploring Simple Siamese Representation Learning. *arXiv preprint arXiv:2011.10566* (2020).
- [7] Y. Chen, X. Zhu, W. Zheng, and J. Lai. 2018. Person Re-Identification by Camera Correlation Aware Feature Augmentation. *IEEE Transactions on Pattern Analysis and Machine Intelligence (TPAMI)* (2018).
- [8] Jia Deng, Wei Dong, Richard Socher, Li-Jia Li, Kai Li, and Li Fei-Fei. 2009. Imagenet: A large-scale hierarchical image database. In *IEEE conference on computer vision and pattern recognition (CVPR)*.
- [9] Jiankang Deng, Jia Guo, Niannan Xue, and Stefanos Zafeiriou. 2019. Arcface: Additive angular margin loss for deep face recognition. In *Proceedings of the IEEE Conference on Computer Vision and Pattern Recognition (CVPR)*.
- [10] Laurent Dinh, David Krueger, and Yoshua Bengio. 2014. Nice: Non-linear independent components estimation. *arXiv preprint arXiv:1410.8516* (2014).
- [11] Laurent Dinh, Jascha Sohl-Dickstein, and Samy Bengio. 2016. Density estimation using real nvp. *arXiv preprint arXiv:1605.08803* (2016).
- [12] Jeff Donahue and Karen Simonyan. 2019. Large scale adversarial representation learning. *arXiv preprint arXiv:1907.02544* (2019).
- [13] Mathieu Germain, Karol Gregor, Iain Murray, and Hugo Larochelle. 2015. MADE: Masked Autoencoder for Distribution Estimation. In *Proceedings of The 32nd International Conference on Machine Learning (ICML)*.
- [14] Douglas Gray and Hai Tao. 2008. Viewpoint Invariant Pedestrian Recognition with an Ensemble of Localized Features. In *European Conference on Computer Vision (ECCV)*.
- [15] Jean-Bastien Grill, Florian Strub, Florent Althé, Corentin Tallec, Pierre H Richemond, Elena Buchatskaya, Clément Doersch, Bernardo Avila Pires, Zhaoan Daniel Guo, Mohammad Gheshlaghi Azar, et al. 2020. Bootstrap your own latent: A new approach to self-supervised learning. *arXiv preprint arXiv:2006.07733* (2020).
- [16] Kaiming He, Haoqi Fan, Yuxin Wu, Saining Xie, and Ross Girshick. 2020. Momentum contrast for unsupervised visual representation learning. In *Proceedings of the IEEE Conference on Computer Vision and Pattern Recognition (CVPR)*.
- [17] Kaiming He, Xiangyu Zhang, Shaoqing Ren, and Jian Sun. 2016. Deep residual learning for image recognition. In *Proceedings of the IEEE conference on computer vision and pattern recognition (CVPR)*.
- [18] Lingxiao He, Xingyu Liao, Wu Liu, Xinchun Liu, Peng Cheng, and Tao Mei. 2020. FastReID: a Pytorch toolbox for real-world person re-identification. *arXiv preprint arXiv:2006.02631* (2020).
- [19] Sergey Ioffe and Christian Szegedy. 2015. Batch normalization: Accelerating deep network training by reducing internal covariate shift. In *International conference on machine learning (ICML)*.
- [20] Diederik P Kingma and Jimmy Ba. 2014. Adam: A method for stochastic optimization. *arXiv preprint arXiv:1412.6980* (2014).
- [21] Diederik P Kingma and Prafulla Dhariwal. 2018. Glow: Generative flow with invertible 1x1 convolutions. *arXiv preprint arXiv:1807.03039* (2018).
- [22] Martin Köstinger, Martin Hirzer, Paul Wohlhart, Peter M Roth, and Horst Bischof. 2012. Large scale metric learning from equivalence constraints. In *IEEE Conference on Computer Vision and Pattern Recognition (CVPR)*.
- [23] Gustav Larsson, Michael Maire, and Gregory Shakhnarovich. 2016. Learning representations for automatic colorization. In *European conference on computer vision (ECCV)*.
- [24] Christian Ledig, Lucas Theis, Ferenc Huszár, José Caballero, Andrew Cunningham, Alejandro Acosta, Andrew Aitken, Alykhan Tejani, Johannes Totz, Zehan Wang, et al. 2017. Photo-realistic single image super-resolution using a generative adversarial network. In *IEEE conference on computer vision and pattern recognition (CVPR)*.
- [25] Hanjun Li, Gaojie Wu, and Wei-Shi Zheng. 2021. Combined Depth Space based Architecture Search For Person Re-identification. *arXiv preprint arXiv:2104.04163* (2021).
- [26] Minxian Li, Xiatian Zhu, and Shaogang Gong. 2018. Unsupervised person re-identification by deep learning tracklet association. In *Proceedings of the European conference on computer vision (ECCV)*.
- [27] Wei Li, Rui Zhao, Tong Xiao, and Xiaogang Wang. 2014. DeepReID: Deep Filter Pairing Neural Network for Person Re-identification. In *IEEE Conference on Computer Vision and Pattern Recognition (CVPR)*.
- [28] Wei Li, Xiatian Zhu, and Shaogang Gong. 2018. Harmonious Attention Network for Person Re-identification. In *IEEE Conference on Computer Vision and Pattern Recognition (CVPR)*.
- [29] Shengcai Liao, Yang Hu, Xiangyu Zhu, and Stan Z Li. 2015. Person re-identification by Local Maximal Occurrence representation and metric learning. In *IEEE Conference on Computer Vision and Pattern Recognition (CVPR)*.
- [30] Weiyang Liu, Yandong Wen, Zhiding Yu, Ming Li, Bhiksha Raj, and Le Song. 2017. SpheroFace: Deep hypersphere embedding for face recognition. In *Proceedings of the IEEE conference on computer vision and pattern recognition (CVPR)*.
- [31] Zimo Liu, Jingya Wang, Shaogang Gong, Huchuan Lu, and Dacheng Tao. 2019. Deep Reinforcement Active Learning for Human-in-the-Loop Person Re-Identification. In *The IEEE International Conference on Computer Vision (ICCV)*.
- [32] Mingsheng Long, Yue Cao, Jianmin Wang, and Michael Jordan. 2015. Learning transferable features with deep adaptation networks. In *International conference on machine learning (ICML)*.
- [33] Hao Luo, Youzhi Gu, Xingyu Liao, Shenqi Lai, and Wei Jiang. 2019. Bag of tricks and a strong baseline for deep person re-identification. In *Proceedings of the IEEE Conference on Computer Vision and Pattern Recognition Workshops (CVPR)*.
- [34] Wenhan Luo, Björn Stenger, Xiaowei Zhao, and Tae-Kyun Kim. 2018. Trajectories as topics: Multi-object tracking by topic discovery. *IEEE Transactions on Image Processing (TIP)* (2018).
- [35] Lei Qi, Lei Wang, Jing Huo, Yinghuan Shi, and Yang Gao. 2019. Adversarial camera alignment network for unsupervised cross-camera person re-identification. *arXiv preprint arXiv:1908.00862* (2019).
- [36] Lei Qi, Lei Wang, Jing Huo, Yinghuan Shi, and Yang Gao. 2020. Progressive cross-camera soft-label learning for semi-supervised person re-identification. *IEEE Transactions on Circuits and Systems for Video Technology (TCSVT)* (2020).
- [37] Ali Razavi, Aaron van den Oord, and Oriol Vinyals. 2019. Generating diverse high-fidelity images with vq-vae-2. *arXiv preprint arXiv:1906.00446* (2019).
- [38] Arulkumar Subramaniam, Moitreyee Chatterjee, and Anurag Mittal. 2016. Deep Neural Networks with Inexact Matching for Person Re-Identification. In *Advances in Neural Information Processing Systems (NeurIPS)*.
- [39] Yumin Suh, Jingdong Wang, Siyu Tang, Tao Mei, and Kyoung Mu Lee. 2018. Part-aligned bilinear representations for person re-identification. In *Proceedings of the European Conference on Computer Vision (ECCV)*.
- [40] Baochen Sun and Kate Saenko. 2016. Deep coral: Correlation alignment for deep domain adaptation. In *European conference on computer vision (ECCV)*.
- [41] Yifan Sun, Liang Zheng, Yi Yang, Qi Tian, and Shengjin Wang. 2018. Beyond part models: Person retrieval with refined part pooling (and a strong convolutional baseline). In *Proceedings of the European conference on computer vision (ECCV)*.
- [42] Yonglong Tian, Chen Sun, Ben Poole, Dilip Krishnan, Cordelia Schmid, and Phillip Isola. 2020. What makes for good views for contrastive learning. *arXiv preprint arXiv:2005.10243* (2020).
- [43] Laurens Van der Maaten and Geoffrey Hinton. 2008. Visualizing data using t-SNE. *Journal of machine learning research (JMLR)* (2008).
- [44] Ashish Vaswani, Noam Shazeer, Niki Parmar, Jakob Uszkoreit, Llion Jones, Aidan N Gomez, Lukasz Kaiser, and Illia Polosukhin. 2017. Attention is all you need. *arXiv preprint arXiv:1706.03762* (2017).
- [45] Guanshuo Wang, Yufeng Yuan, Xiong Chen, Jiwei Li, and Xi Zhou. 2018. Learning discriminative features with multiple granularities for person re-identification. In *Proceedings of the 26th ACM international conference on Multimedia (ACMMM)*.
- [46] Menglin Wang, Baisheng Lai, Haokun Chen, Jianqiang Huang, Xiaojin Gong, and Xian-Sheng Hua. 2021. Towards precise intra-camera supervised person re-identification. In *Proceedings of the IEEE Winter Conference on Applications of Computer Vision (WACV)*.
- [47] Taiqing Wang, Shaogang Gong, Xiatian Zhu, and Shengjin Wang. 2014. Person re-identification by video ranking. In *European Conference on Computer Vision (ECCV)*.
- [48] Taiqing Wang, Shaogang Gong, Xiatian Zhu, and Shengjin Wang. 2016. Person Re-Identification by Discriminative Selection in Video Ranking. *IEEE Transactions on Pattern Analysis and Machine Intelligence (TPAMI)* (2016).
- [49] Longhui Wei, Shiliang Zhang, Wen Gao, and Qi Tian. 2018. Person transfer gan to bridge domain gap for person re-identification. In *IEEE Conference on Computer Vision and Pattern Recognition (CVPR)*.
- [50] Yandong Wen, Kaipeng Zhang, Zhifeng Li, and Yu Qiao. 2016. A discriminative feature learning approach for deep face recognition. In *European conference on computer vision (ECCV)*.
- [51] Guile Wu, Xiatian Zhu, and Shaogang Gong. 2020. Tracklet self-supervised learning for unsupervised person re-identification. In *Proceedings of the AAAI Conference on Artificial Intelligence (AAAI)*.
- [52] Jinlin Wu, Yang Yang, Hao Liu, Shengcai Liao, Zhen Lei, and Stan Z Li. 2019. Unsupervised graph association for person re-identification. In *IEEE International Conference on Computer Vision (ICCV)*.

- [53] Tong Xiao, Hongsheng Li, Wanli Ouyang, and Xiaogang Wang. 2016. Learning Deep Feature Representations with Domain Guided Dropout for Person Re-identification. In *IEEE Conference on Computer Vision and Pattern Recognition (CVPR)*.
- [54] Fei Xiong, Mengran Gou, Octavia Camps, and Mario Sznai. 2014. Person re-identification using kernel-based metric learning methods. In *European Conference on Computer Vision (ECCV)*.
- [55] Mang Ye, Jianbing Shen, Gaojie Lin, Tao Xiang, Ling Shao, and Steven CH Hoi. 2021. Deep learning for person re-identification: A survey and outlook. *IEEE Transactions on Pattern Analysis and Machine Intelligence (TPAMI)* (2021).
- [56] Tianyu Zhang, Lingxi Xie, Longhui Wei, Yongfei Zhang, Bo Li, and Qi Tian. 2020. Single camera training for person re-identification. In *Proceedings of the AAAI Conference on Artificial Intelligence (AAAI)*.
- [57] Liang Zheng, Liyue Shen, Lu Tian, Shengjin Wang, Jingdong Wang, and Qi Tian. 2015. Scalable Person Re-identification: A Benchmark. In *IEEE International Conference on Computer Vision (ICCV)*.
- [58] Liang Zheng, Liyue Shen, Lu Tian, Shengjin Wang, Jingdong Wang, and Qi Tian. 2015. Scalable person re-identification: A benchmark. In *IEEE International Conference on Computer Vision (ICCV)*.
- [59] Wei-Shi Zheng, Shaogang Gong, and Tao Xiang. 2013. Reidentification by Relative Distance Comparison. *IEEE Transactions on Pattern Analysis and Machine Intelligence (TPAMI)* (2013).
- [60] Zhedong Zheng, Liang Zheng, and Yi Yang. 2017. Unlabeled Samples Generated by GAN Improve the Person Re-identification Baseline in Vitro. In *2017 IEEE International Conference on Computer Vision (ICCV)*.
- [61] Zhun Zhong, Liang Zheng, Shaozi Li, and Yi Yang. 2018. Generalizing a person retrieval model hetero-and homogeneously. In *Proceedings of the European Conference on Computer Vision (ECCV)*.
- [62] Xiangping Zhu, Xiatian Zhu, Minxian Li, Vittorio Murino, and Shaogang Gong. 2019. Intra-camera supervised person re-identification: A new benchmark. In *IEEE International Conference on Computer Vision Workshops (ICCV)*.
- [63] Zijie Zhuang, Longhui Wei, Lingxi Xie, Haizhou Ai, and Qi Tian. 2021. Camera-based Batch Normalization: An Effective Distribution Alignment Method for Person Re-identification. *IEEE Transactions on Circuits and Systems for Video Technology(TCSVT)* (2021).
- [64] Zijie Zhuang, Longhui Wei, Lingxi Xie, Tianyu Zhang, Hengheng Zhang, Haozhe Wu, Haizhou Ai, and Qi Tian. 2020. Rethinking the distribution gap of person re-identification with camera-based batch normalization. In *European Conference on Computer Vision (ECCV)*.